

# On the strength of hydrogen bonding within water clusters on the coordination limit

Víctor Manuel Castor-Villegas<sup>a</sup>, José Manuel Guevara-Vela<sup>a</sup>, Wilmer E. Vallejo Narváez<sup>b</sup>,  
Ángel Martín Pendás<sup>c</sup>, Alberto Fernández-Alarcón<sup>a,\*</sup>, Tomás Rocha-Rinza<sup>a,\*</sup>

<sup>a</sup>*Institute of Chemistry, National Autonomous University of Mexico, Circuito Exterior, Ciudad Universitaria, Delegación Coyoacán C.P. 04510, Mexico City, Mexico.*

<sup>b</sup>*Institute of Materials, National Autonomous University of Mexico, Circuito Exterior, Ciudad Universitaria, Delegación Coyoacán C.P. 04510, Mexico City, Mexico.*

<sup>c</sup>*Department of Analytical and Physical Chemistry, University of Oviedo, E-33006, Oviedo, Spain.*

---

## Abstract

Hydrogen bonds (HB) are arguably the most important non-covalent interactions in chemistry. We study herein how differences in connectivity alter the strength of HBs within water clusters of different sizes. We used for this purpose the interacting quantum atoms (IQA) topological energy partition, a methodology that allows for the quantification of the interaction energy among molecules within a molecular cluster. We classified monomers within H<sub>2</sub>O clusters according to their connectivity and we could expand our previously reported hierarchy of HB strength in these systems (*Phys. Chem. Chem. Phys.*, 2016, **18**, 19557) to include tetracoordinated monomers. Our results show that the formation energies of HBs between tetracoordinated water molecules are slightly lower than specific arrangements of tricoordinated H<sub>2</sub>O monomers. Nonetheless, HB tetracoordination is preferred because (i) it strengthens HBs associated with the occurrence of double HB donors and acceptors and (ii) it allows for the occurrence of a larger number of favourable interactions in the system. Although tetracoordination increases total number of contacts, it may also weaken or strengthen other HBs. Moreover, we found that the strongest and weakest HBs are formed by tricoordinated monomers with favorable and unfavorable connectivity, respectively, while the contacts between tetracoordinated water molecules are on the middle of this scale. Overall, we expect that this investigation will provide

---

\*To whom correspondence should be addressed: al.fedza@gmail.com, trocha@iquimica.com.mx

valuable insights on the subtle interplay of tri- and tetracoordination and acceptors and the resulting interaction energies within H<sub>2</sub>O clusters.

*Keywords:*

Water clusters, IQA, Hydrogen bonding, Coordination number

---

## Introduction

Hydrogen bonds (HB) are critical in a wide variety of fields, such as molecular recognition [1] and catalysis. [2] Hence, the understanding of the nature of HBs is an active research avenue in constant development. The correct characterisation of HB is a complicated endeavour whose principal difficulties lie in the description of the non-additive contributions to this interaction. In other words, the proper account of HBs entails the understanding of how HBs affect each other increasing (cooperativity) or decreasing (anticooperativity) their formation energies. [3, 4]

Water clusters are valuable archetypes for the study of HB non-additivity. [5–7] The cooperative and anticooperative behaviour of HBs in H<sub>2</sub>O clusters depends on the connectivity of the monomers involved in the interaction, i.e., whether they are single or double proton donor or acceptors. For example, homodromic networks of HBs (Figure 1(a)), particularly in small water clusters, are related with strong HB cooperative effects. The dependency of HB formation energies on connectivity motivated some of us to propose a scale of HB strength based on the single/double and acceptor/donor character of water molecules in H<sub>2</sub>O clusters. [4] This hierarchy of HB strength illustrates important features of hydrogen bonding within water clusters, for instance, the fact that double donors or acceptors are related not only with HB anticooperativity (Figure 1(b)), as previously suggested, [8] but also with HB cooperative effects. Despite its correct account of relative HB formation energies within small water clusters, this scale of HB strength in H<sub>2</sub>O adducts is incomplete because it does not include tetracoordinated water molecules, which is an important arrangement of H<sub>2</sub>O molecules in large water clusters as well as liquid and solid water.

We intend to contribute further in this direction by examining formation energies within water clusters with tetracoordinated monomers using Quantum Chemical Topology (QCT) tools.

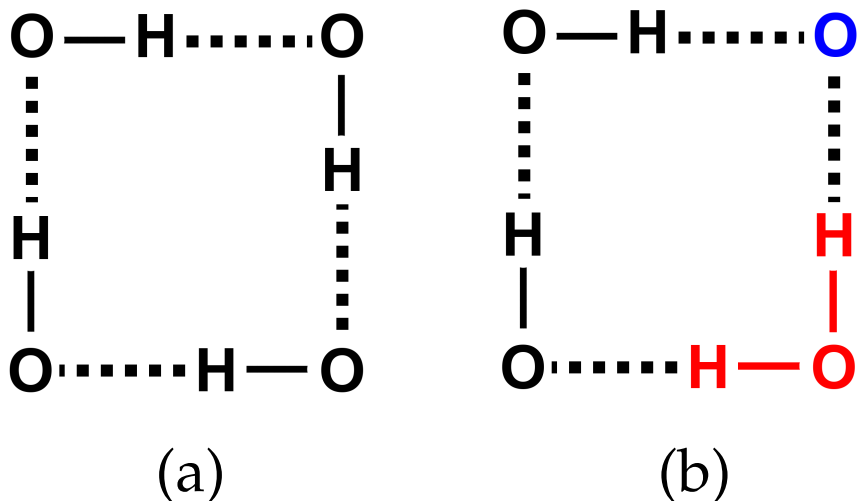


Figure 1: Homodromic (a) and antidromic (b) cycles formed by water molecules. The double HB donor and acceptor species in (b) are highlighted in red and blue, respectively.

QCT comprises a set of methodologies that use the language of dynamical systems to partition and to characterise molecules and molecular complexes via the topological analysis of several scalar fields derived from the electronic wave function. [9, 10] The methods in QCT have the attractive feature of being invariant to orbital transformations and they are robust against the change of the level of approximation in electronic structure theory. [11] QCT analyses have been used to investigate a variety of non-covalent interactions such as  $\pi$ - $\pi$  [12] and  $\sigma$ - $\sigma$  stacking, [13], chalcogen contacts [14], or pnictogen bonds. [15–17] Two of the methods within QCT that has been very successful in this regard are (i) the Quantum Theory of Atoms in Molecules (QTAIM) based on the topology of the electron density and (ii) the Interacting Quantum Atoms (IQA) approach, a rigorous partition of the electronic energy based solely on the vector state of the system. [18] Different workers have exploited QTAIM and IQA to study halogen [19–22], beryllium, [23, 24] and tetrel bonding [25] to name a few. Most importantly for this work, the use of QTAIM and IQA has provided valuable insights in the understanding of HBs. [3, 4, 26–28]

Given the main aim of this investigation, this paper is organised as follow. First, we present

the theoretical framework of the methods exploited in this investigation and the associated computational details of our calculations. Later on, we summarise and discuss our principal results. Finally, we enumerate our main conclusions. Briefly, we were able to expand our previously reported scale for the strength of HBs with the inclusion of tetracoordinated water molecules. We found that the HB formation energies involving tetracoordinated water monomers do not correspond to the strongest HB arrangement as it could have been anticipated given the predominance of these motifs of water molecules for example in ice  $I_h$ . Despite its smaller formation energy, tetracoordination is favoured in large  $H_2O$  clusters and in the bulk because (i) it reduces HB anticooperativity due to double HB donors or acceptors (ii) it increases the number of attractive interactions in these molecular adducts. Overall, we expect that this contribution provides important insights about the complex relationship between the connectivity of  $H_2O$  monomers within a cluster and the energies associated to the resulting interactions.

## Theoretical framework

The foundations of QCT were laid out by the development of the QTAIM by Bader and coworkers. [29] The QTAIM is built on the topological examination of the electron density which leads us to recover key chemical concepts, such as atoms, functional groups and chemical bonding from quantum chemical calculations. Additionally, the QTAIM defines a division of the 3D space in atomic basins, i.e., proper quantum subsystems for which we can compute average values of Dirac observables, such as the atomic energy and different atomic multipole moments. [30] Moreover, the QTAIM also defines the delocalisation of the electrons of a basin A into another atom B, an indicator of the degree of covalency between these atoms. [31]

Based on the topological division of the 3D defined by QTAIM, the IQA methodology [18, 32] performs a division of the electronic energy of a molecule or molecular cluster using the first and second order density matrices of the investigated system. The IQA methodology can be also employed within the formalism of Kohn-Sham theory, [33, 34] despite the lack of second order densities in DFT. More specifically, the IQA analysis conduces to a separation of the electronic energy in intraatomic,  $E_{\text{net}}^A$ , and interatomic,  $E_{\text{int}}^{AB}$ , components, [18, 32]

$$E = \sum_A E_{\text{net}}^A + \frac{1}{2} \sum_A \sum_{B \neq A} E_{\text{int}}^{\text{AB}}, \quad (1)$$

wherein A, B, ... are the atomic basins defined by the QTAIM. The intra and interatomic contributions can be further decomposed as

$$E_{\text{net}}^A = T^A + V_{\text{ne}}^{\text{AA}} + V_{\text{ee}}^{\text{AA}}, \quad (2)$$

and

$$E_{\text{int}}^{\text{AB}} = V_{\text{nn}}^{\text{AB}} + V_{\text{ne}}^{\text{AB}} + V_{\text{ne}}^{\text{BA}} + V_{\text{ee}}^{\text{AB}}, \quad (3)$$

with  $T^A$  being the kinetic energy of atom A, while  $V_{\text{ne}}^{\text{AB}}$  and  $V_{\text{ee}}^{\text{AB}}$  represent (i) the attraction of the nucleus of atom A with the electrons of the basin B and (ii) the repulsion of the electrons of the same atoms. Finally,  $V_{\text{nn}}^{\text{AB}}$  denotes the repulsion between the nuclei of atoms A and B.

We can also divide the IQA interaction energy between two atoms into classical ( $V_{\text{cl}}^{\text{AB}}$ ) and exchange-correlation ( $V_{\text{xc}}^{\text{AB}}$ ) contributions,

$$E_{\text{int}}^{\text{AB}} = V_{\text{cl}}^{\text{AB}} + V_{\text{xc}}^{\text{AB}}. \quad (4)$$

The terms  $V_{\text{cl}}^{\text{AB}}$  and  $V_{\text{xc}}^{\text{AB}}$  are commonly identified with ionic and covalent components of the interaction energy between atoms A and B, respectively. The conceptual framework of IQA enables us to regroup the terms of equation (1) to express the corresponding values of the net and interaction energies for groups of atoms,  $\mathcal{G}$ ,  $\mathcal{H}$ ,  $\mathcal{I}$ , within an electronic system, e.g. monomers forming a molecular cluster,

$$E = \sum_{\mathcal{G}} E_{\text{net}}^{\mathcal{G}} + \frac{1}{2} \sum_{\mathcal{G}} \sum_{\mathcal{G} \neq \mathcal{H}} E_{\text{int}}^{\mathcal{GH}}, \quad (5)$$

in which

$$E_{\text{net}}^{\mathcal{G}} = \sum_{A \in \mathcal{G}} E_{\text{net}}^A + \frac{1}{2} \sum_{A \in \mathcal{G}} \sum_{\substack{B \in \mathcal{G} \\ B \neq A}} E_{\text{int}}^{\text{AB}}. \quad (6)$$

and

$$E_{\text{int}}^{\mathcal{GH}} = \sum_{A \in \mathcal{G}} \sum_{B \in \mathcal{H}} E_{\text{int}}^{\text{AB}} \quad (7)$$

Finally, it is possible to represent the changes in energy associated with the formation of a molecular cluster,  $\mathcal{G} + \mathcal{H} + \mathcal{G} \rightleftharpoons \mathcal{G} \cdots \mathcal{H} \cdots \mathcal{G}$ , as the sum:

$$\Delta E = \sum_{\mathcal{G}} E_{\text{def}}^{\mathcal{G}} + \sum_{\mathcal{G}} \sum_{\mathcal{G} > \mathcal{H}} E_{\text{int}}^{\mathcal{GH}}, \quad (8)$$

wherein  $E_{\text{def}}^{\mathcal{G}}$ , denotes the deformation energy of group  $\mathcal{G}$ , namely the difference in energy between  $\mathcal{G}$  within the molecular cluster (computed with Eq. (6)) and isolated in its equilibrium geometry. [18]. We can rewrite equation (8) as a pairwise sum of interacting monomers [4]

$$\begin{aligned} \Delta E &= \sum_{\mathcal{G}} \sum_{\mathcal{G} > \mathcal{H}} \left( E_{\text{int}}^{\mathcal{GH}} + \left( \frac{E_{\text{int}}^{\mathcal{GH}}}{\sum_{\mathcal{J} \neq \mathcal{G}} E_{\text{int}}^{\mathcal{JG}}} \right) E_{\text{def}}^{\mathcal{G}} + \left( \frac{E_{\text{int}}^{\mathcal{GH}}}{\sum_{\mathcal{J} \neq \mathcal{H}} E_{\text{int}}^{\mathcal{JH}}} \right) E_{\text{def}}^{\mathcal{H}} \right) \\ &= \sum_{\mathcal{G}} \sum_{\mathcal{G} > \mathcal{H}} E_{\text{int}}^{\mathcal{GH}'}. \end{aligned} \quad (9)$$

in which  $E_{\text{int}}^{\mathcal{GH}'}$  includes  $E_{\text{int}}^{\mathcal{GH}}$  and a fraction of  $E_{\text{def}}^{\mathcal{G}}$  and  $E_{\text{def}}^{\mathcal{H}}$ . Finally, it is also possible to partition the energy arising from equation (9),  $E_{\text{int}}^{\mathcal{GH}'}$  into classical and exchange-correlation components,

$$\begin{aligned} \Delta E &= \sum_{\mathcal{G}} \sum_{\mathcal{G} > \mathcal{H}} (E_{\text{xc}}^{\mathcal{GH}} + E_{\text{class}}^{\mathcal{GH}}) \left( 1 + \left( \frac{1}{\sum_{\mathcal{J} \neq \mathcal{G}} E_{\text{int}}^{\mathcal{JG}}} \right) E_{\text{def}}^{\mathcal{G}} + \left( \frac{1}{\sum_{\mathcal{J} \neq \mathcal{H}} E_{\text{int}}^{\mathcal{JH}}} \right) E_{\text{def}}^{\mathcal{H}} \right) \\ &= \sum_{\mathcal{G}} \sum_{\mathcal{G} > \mathcal{H}} (E_{\text{xc}}^{\mathcal{GH}'} + E_{\text{cl}}^{\mathcal{GH}'}) \end{aligned} \quad (10)$$

### *Computational details*

We optimised the structures of sixteen water clusters  $(\text{H}_2\text{O})_n$   $n = 6 \dots 17$ , shown in Figure 2. The starting geometries of the examined systems were taken from the literature [35–37] and recomputed with the M06-2x/6-311++G(d,p) approximation. [38, 39] Later on, single point calculations were performed at the M06-2x/aug-cc-pVTZ [40, 41] level of theory. All these calculations were carried out using the package GAUSSIAN09 [42]. We decided to employ this methodology because the combination of this exchange-correlation functional with basis sets of triple-zeta quality reproduces adequately the cooperative and anticooperative behaviour described by correlated wavefunctions at a moderate computational cost. [43] Later on, using the electronic densities computed via DFT we proceeded to analyse the QTAIM topological properties of the electron density and to carry out the IQA energy partition. [33, 34] We used the AIMALL program for these purposes. [44]. The visualisation of our results were carried out with the help of the GAUSVIEW program [42] and the MATPLOTLIB [45] library.

### **Results and discussions**

As stated in the Introduction, we had previously suggested a scale for the strength of HBs between water molecules based on the single and double character of the involved hydrogen bond donors and acceptors. [4] This scale is incomplete, however, because it does not include tetracoordinated water monomers. By considering the systems show in Figure 2, we were able to ameliorate this omission. Table 1 gives a description of the ten categories in which we separated the different types of HBs within water clusters. This new scale includes the six types of HB considered before [4] as well as four new categories which entail tetracoordinated water molecules. The types of HB in Table 1 are ordered from less energetic (1) to more energetic (10). The averages of the formation energies between water molecules for the different types of HB are presented in Figure 3. These values span from  $4.9 \pm 0.8$  to  $8.0 \pm 0.5$  kcal/mol. We recall at this point the binding energy computed with the M06-2x/aug-cc-pVTZ approximation is  $-5.2$  kcal mol<sup>-1</sup>. Thus hydrogen bond formation energies within water clusters can be reduced by  $\approx 25\%$  (anticooperativity) or increased by  $\approx 65\%$  (cooperativity). Figure 3 also presents the

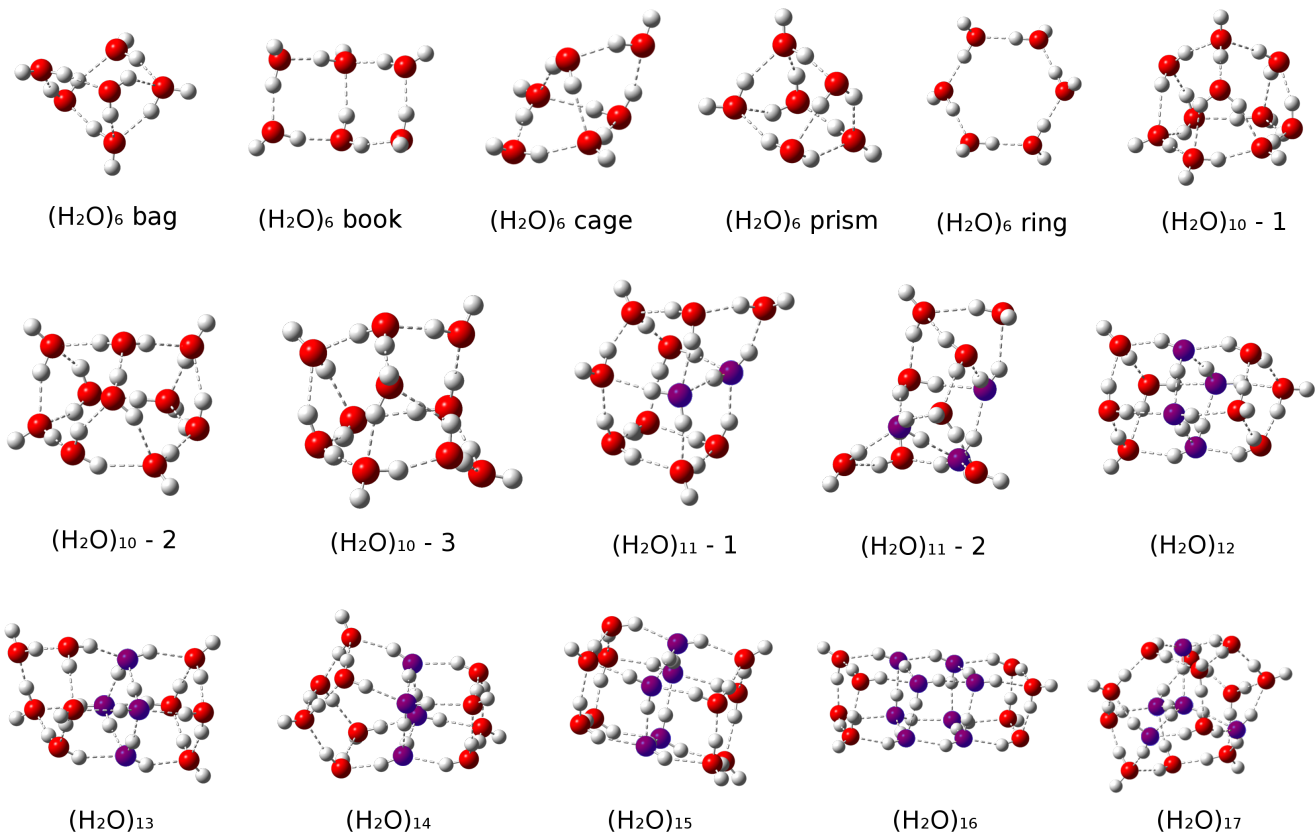


Figure 2: Water clusters considered in this work. The oxygen atoms corresponding to tetracoordinated molecules are highlighted in purple.

fomerly suggested scale in reference [4] in red. We point out the good agreement between the old and new data, in particular considering that the previous work relied on MP2/aug-cc-pVTZ electronic structure calculations. We note an inversion for the order of the hydrogen bond types (4) and (5) of the previous scale. But we also point out that the formation energies of these HBs in the previous scale are very similar  $-7.01$  and  $-6.96$  kcal/mol. This observation is consistent with previous reports which state that the description of HB cooperativity and anticooperativity is robust with respect to changes in different approximations in electronic structure theory. [43]

Figure 3 shows that the interaction between two tetracoordinated molecules, type number



(6), lies in the middle of the scale. Thus, we can say that tetracoordinated molecules are close to what can be considered close to the average of the hydrogen bond formation within water clusters. The arithmetic mean of the computed formation energies is  $-6.0$  kcal/mol and it corresponds to HB (5) ( $-6.0 \pm 0.6$ ) while that for two tetracoordinated molecules is ( $-6.3 \pm 0.4$ ) kcal/mol. Other categories that include tetracoordinated molecules are (2), (3), and (7).

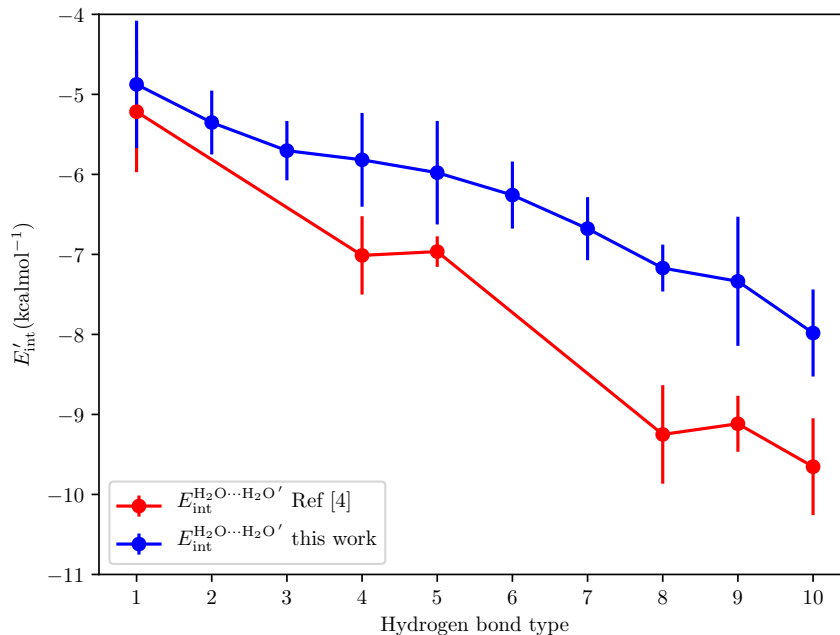


Figure 3: Distribution of IQA formation energies,  $E'_{\text{int}}{}^{\text{H}_2\text{O}\cdots\text{H}_2\text{O}'}$  (eqn (9)) between hydrogen-bonded water molecules for the types of hydrogen bonds described in in Table 1.

Espinosa et. al. suggested to estimate the formation energy corresponding to an HB by using the expression [46]

$$E_{\text{HB}} \approx 0.5V(\mathbf{r}_{\text{bcp}}), \quad (11)$$

where  $\mathbf{r}_{\text{bcp}}$  is the position of the bond critical point associated to the HB, and  $V$  the potential energy density at that critical point. Figure 4 shows the values corresponding to this estimation

Table 1: Scale of hydrogen bond formation energies within water clusters put forward in this investigation. The hierarchy is presented in an increasing order of magnitude of the H-bond formation energies.

Type of HB	Description
(1)	( <i>i</i> ) the H atom involved in the hydrogen bond belongs to a molecule which is a double HB donor and ( <i>ii</i> ) the oxygen that participates in the interaction is a double HB acceptor.
(2)	a tetracoordinated water molecule either ( <i>i</i> ) donates an HB to a double HB acceptor or ( <i>ii</i> ) accepts an HB from a double HB donor.
(3)	a tetracoordinated water molecule interacts with a monomer which is a single HB donor and a single HB acceptor.
(4)	a hydrogen bond is formed between two double HB donors or two double HB acceptors.
(5)	( <i>i</i> ) a hydrogen of a double HB donor is bonded to the oxygen of a single HB acceptor or ( <i>ii</i> ) the oxygen of a double HB acceptor interacts with a hydrogen of a single HB donor.
(6)	Both water molecules are tetracoordinated.
(7)	a tetracoordinated H <sub>2</sub> O molecule either ( <i>i</i> ) donates an HB to a double HB donor or ( <i>ii</i> ) accepts an HB from a double HB acceptor.
(8)	a hydrogen of a single HB donor interacts with the oxygen of a single HB acceptor.
(9)	( <i>i</i> ) a hydrogen of a double HB acceptor is in contact with the oxygen of a single HB donor or ( <i>ii</i> ) the O atom of a double HB donor interacts with a hydrogen of a single HB acceptor.
(10)	the oxygen atom of a double HB donor interacts with a hydrogen atom of a double HB acceptor.

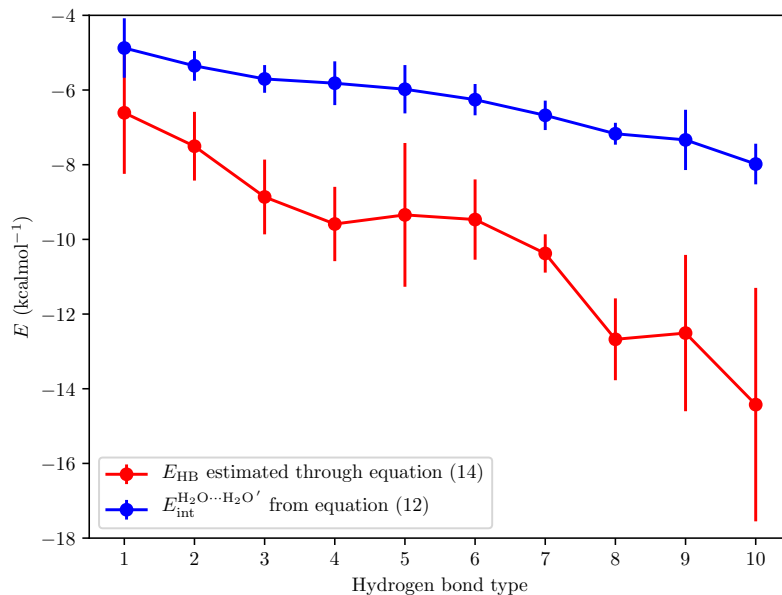


Figure 4: Formation energies of the different types of hydrogen bonds specified in Table 1. The values are reported in kcal mol<sup>-1</sup>.

as well as those of the interaction between water molecules,  $E_{\text{int}}^{\text{H}_2\text{O}\cdots\text{H}_2\text{O}'}$ . As we can appreciate here, in all cases the estimated energy is larger than that computed by IQA. These differences become more pronounced as the HB type becomes more energetic. However, both ways to calculate the hydrogen bond formation energy agree in the order of the different categories given in Table 1.

Interaction energies and distances between molecules tend to follow similar trends. Figure 5 shows the average distances between oxygen atoms for the different types of HBs in the hierarchy put forward in Table 1. We note that O $\cdots$ O distances follow a similar tendency to those shown in Figures 3 and 4. That is to say, longer distances are associated with weaker interactions, while shorter ones are related with stronger contacts as expected.

Figure 5 shows the experimental distance in ice I<sub>h</sub>, [47] marked with a red line. This value is very similar to the average distance of the of HBs in the middle of the scale i.e., those of the (3)–(6) types. Importantly, type (6) corresponds to the interaction between two tetracoordinated

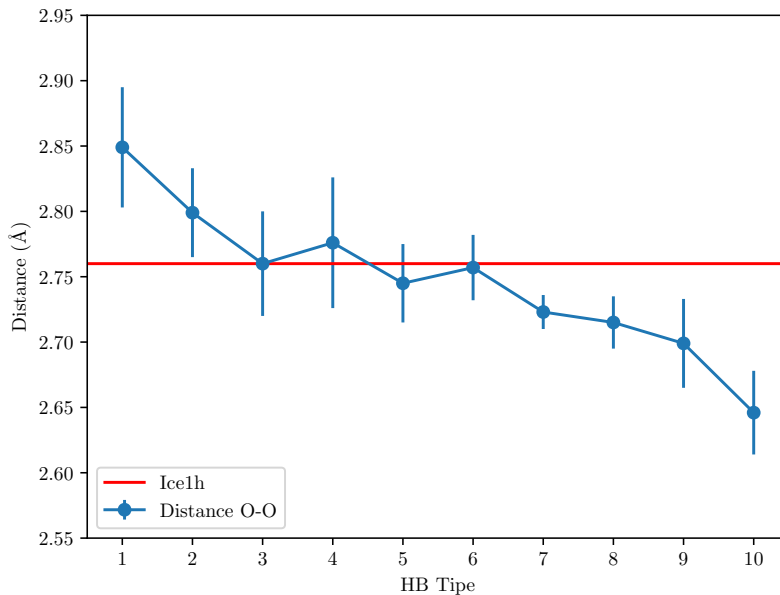


Figure 5: Average distances between oxygen atoms for the different H-bond in Table 1. The values are reported in Å.

molecules, which is the bonding situation observed in this phase of  $\text{H}_2\text{O}$ .

The scale of HB strength suggested herein and that put forward in reference [4] can be rationalized in terms of the charge transfer which occurs in the formation of a hydrogen bond. Because the HBs which take place within water clusters can be considered as incipient Brønsted-Lowry acid-base reactions, [8] there is an electron transfer from the HB acceptor to the HB donor (Figure 6(a)). Such charge transfer strengthen the (i) HB donor capacity of molecule **A** in Figure 6(a), because it has a small positive charge and (ii) the HB acceptor ability of monomer **D** in the same figure, since its oxygen atom is more electron-rich than that in an isolated water molecule. These effects result in hydrogen bond cooperativity, for example within the water trimer shown in Figure 6(b). The charge flow which results from the formation of a hydrogen bond may be also related to hydrogen bond anticooperativity. [8] For example, Figure 6(c) shows a tricoordinated double HB donor for which the electron charge transfer have a twofold effect. First, the two schematised hydrogen bonds in the right of Figure 6(c) weaken each other, i.e., they present HB

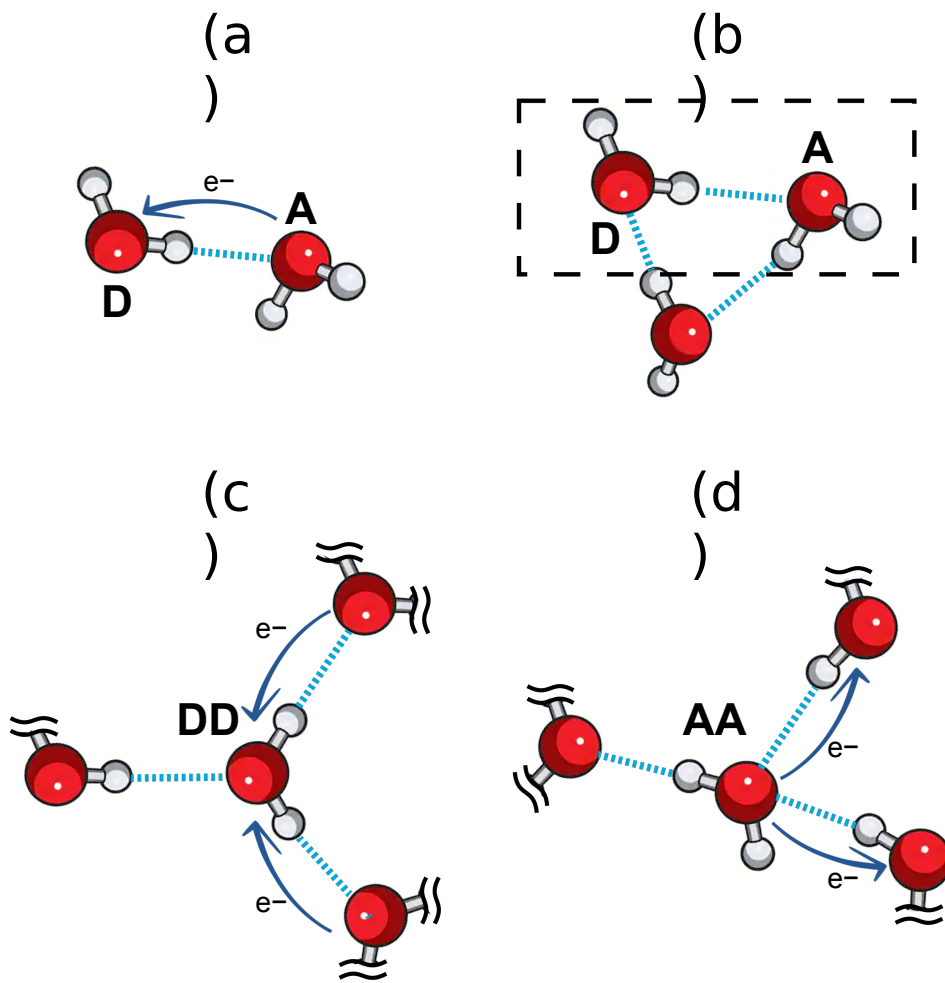
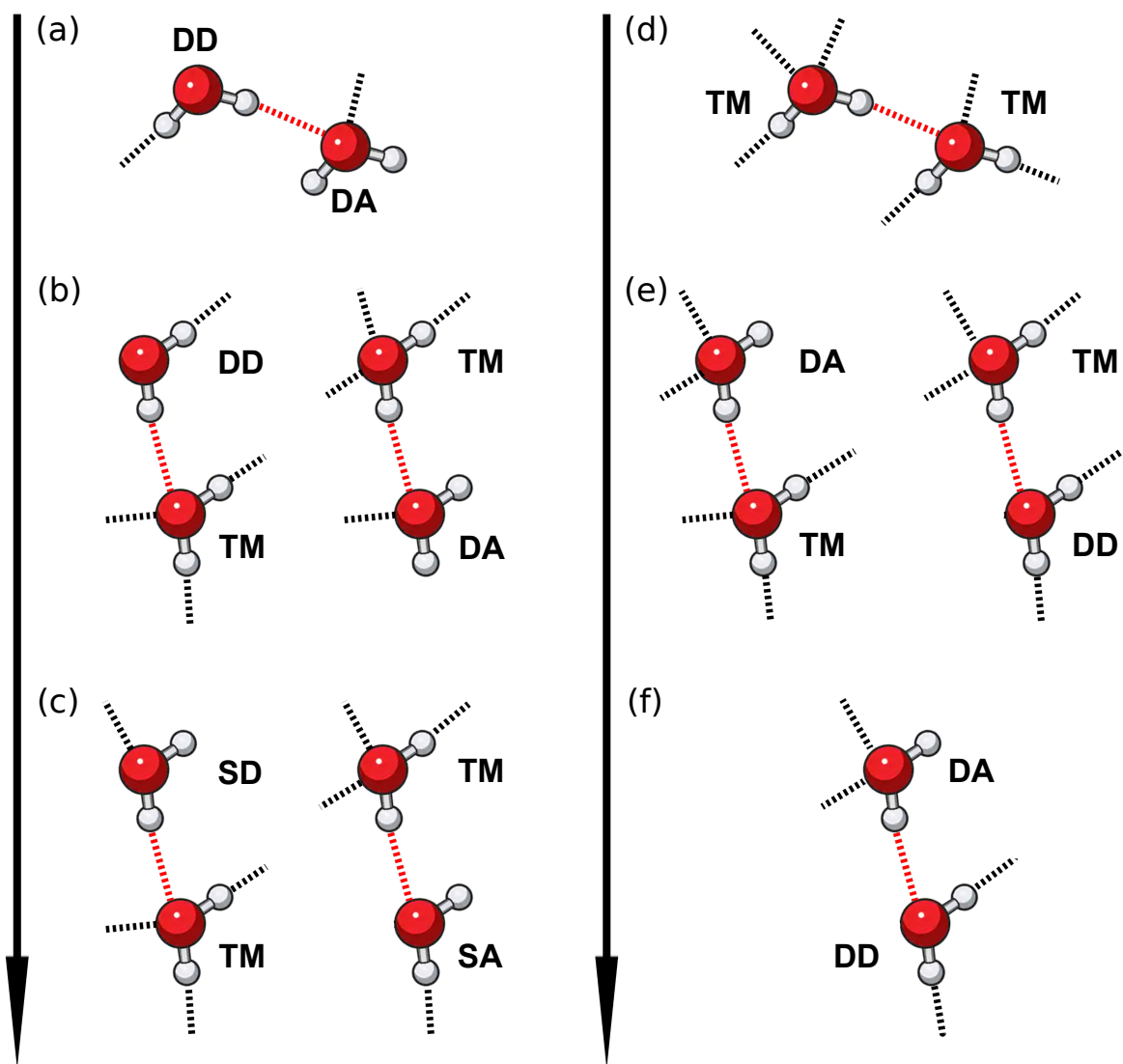


Figure 6: (a) Charge transfer within the water dimer: the molecule **A** donates electron density to the monomer **D** (b) Water trimer. A parent water dimer is highlighted within the inset. The charge transfer described in (a) results in hydrogen bond cooperativity, i.e., the hydrogen bonds within  $(\text{H}_2\text{O})_3$  are stronger than those in  $(\text{H}_2\text{O})_2$  (c) Double hydrogen bond donor. The hydrogen bonds shown in the right of monomer **DD** weaken one another, but their associated charge transfer makes the oxygen of this molecule richer in electrons and strengthen the hydrogen bond in the left of **DD**. (d) Double hydrogen bond acceptor. The hydrogen bonds displayed in the right of molecule **AA** exert anticooperative effects on each other, but the schematised charge transfer makes the protons of **AA** more acidic and therefore more susceptible to form strong hydrogen bonds.

anticooperativity. Second, both charge transfers contribute to make the oxygen atom a better HB acceptor, in a similar fashion to monomer **D** in Figure 6(a). This effect fortifies the HB in the left of Figure 6(c). One may consider that double HB donors are relatively poor HB donors but good HB acceptors. Similar arguments based on charge transfers related to HBs lead to the conclusion that the HBs of the right of Figure 6(d) present anticooperative effects and that the hydrogens of double HB acceptors are more acidic than those of an isolated water monomer and therefore should form stronger HBs than that in  $(\text{H}_2\text{O})_2$ . In other words, double HB donors are comparably poor HB donors but good HB acceptors. Therefore, the weakest type of H-bond in the hierarchy suggested herein involves a double HB donor acting as the HB donor and a double HB acceptor functioning as the HB acceptor in the interaction as displayed in Figure 7(a). On the other hand, the strongest HB on the scale entails a double HB donor operating as the HB acceptor and a double HB acceptor being the corresponding HB donor (Figure 7(f)). Because tetracoordinated water molecules are double HB donors and double HB acceptors, simultaneously, it is difficult to classify them as comparatively good or poor HB donors or acceptors. A similar situation occurs for two-coordinated water molecules which are single HB donors and single HB acceptors. Notwithstanding, Figure 7(b) shows that the weakest type of HB for tetracoordinated water molecules involves poor HB donors. Conversely, the strongest HBs formed by tetracoordinated molecules result from their interactions with the best HB donors (bi- or tricoordinated double HB acceptors) and acceptors (bi- or tricoordinated double HB donors) as shown in Figure 7(e). Figures 7 (c) and (d) represent situations that are intermediates between these two extremes.

The transition from the HB in Figure 7(f), i.e., the strongest of the interactions considered in this investigation, to the HB between two tetracoordinated molecules as schematised in Figure 8 gives valuable insights of the effects of the formation of tetracoordinated water molecules in  $\text{H}_2\text{O}$  clusters. First, when the HB donor **D** in the left of Figure 8 becomes a tetracoordinated molecule, it turns into (i) a worse HB donor and (ii) a better HB acceptor. The first effect weakens the HB indicated in red in Figure 8, but the second consequence strengthens the two HB labelled with the letter *w* (left and middle part of Figure 8). The fortified HBs in Figure



Increase of HB acceptor and donor abilities and hence of HB strength.

Figure 7: Selected hydrogen bonds described in Table 1. (a) and (f) represent the weakest and the strongest types of these interactions in the hierarchy of HB strength put forward in this article. The entries (b)–(e) represent hydrogen bonds which involve at least one tetracoordinated monomer. All the interactions are arranged in an increasing order of H-bond acceptor and donor abilities and therefore of corresponding formation energies. The labels used in the Figure are “DA=Double Acceptor”, “DD=Double Donor”, “TM=Tetracoordinated Monomer”, “SD=Single Acceptor”, “SD=Single Donor”.

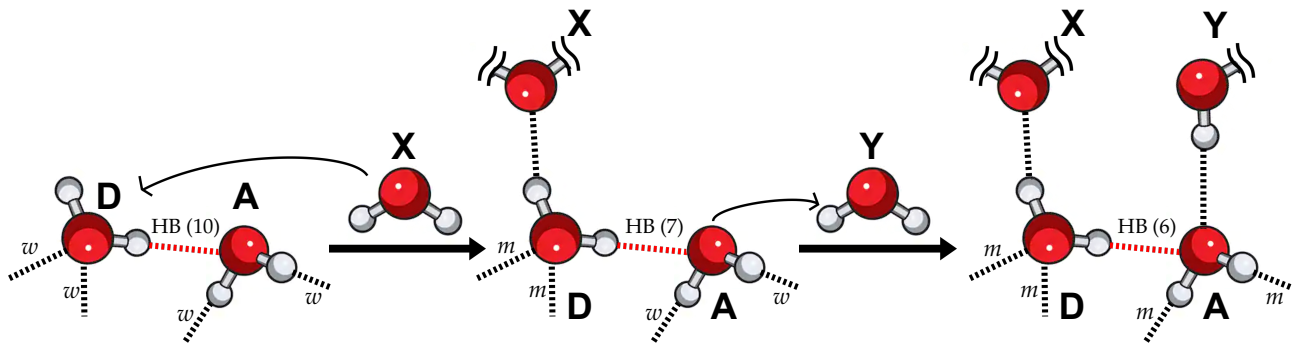
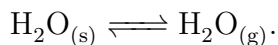


Figure 8: Transition from the strongest type of hydrogen bond in Table 1, namely, HB type (1o) (indicated in red) to the interaction between two tetracoordinated molecules (HB type (6)). The HB type (7) represents an intermediate stage. While the hydrogen bonding indicated in red is weakened by the formation of the two hydrogen bonds those labelled with  $w$  (from “weak”) become stronger as indicated with the letter  $m$  (from “medium force”).

8 are indicated with the letter  $m$ . Likewise, when the fourth HB is formed around molecule A, this monomer becomes (i) a worse HB acceptor and (ii) a better HB donor. These conditions have similar effects than those just mentioned, i.e., the HB indicated in red in Figure 8 is further weakened and the other HBs of **D** become fortified. Overall, tetracoordination allows to increase the number of attractive hydrogen bonds within a system while it might weaken or strengthen other previously formed HBs.

Now, we discuss briefly how the formation energy of the hydrogen bond among tetracoordinated molecules (HB type (6)) can be associated with the sublimation energy of ice:



The formation energy of HB type (6) is  $-6.3 \text{ kcal mol}^{-1}$ . Hence, the break of all HBs in ice (composed of tetracoordinated molecules) would equal twice this quantity, i.e.,  $-12.6 \text{ kcal mol}^{-1}$ , by ignoring three and many-body effects. The sublimation of ice at 0 K is  $11.4 \text{ kcal mol}^{-1}$  [48] which is in a reasonably good agreement with the estimated value based on the HB formation energies of tetracoordinated molecules.



*Covalent vs ionic components of  $E_{\text{int}}^{\text{H}_2\text{O}\cdots\text{H}_2\text{O}'}$*

Finally, the IQA energy partition is able to divide the HB formation energy in classical (ionic) and exchange-correlation (covalent) parts. Figure 9 shows the values for these contributions to the interaction energy between water molecules for the different types of hydrogen bonds in the scale of Table 1. The values for the classical term,  $E_{\text{class}}^{\text{H}_2\text{O}\cdots\text{H}_2\text{O}'}$ , are quite similar for all types of HBs in this hierarchy. On the contrary, the differences for the exchange-correlation term,  $E_{\text{xc}}^{\text{H}_2\text{O}\cdots\text{H}_2\text{O}'}$ , are larger. Thus, we can say that the variations in the total interaction energy come almost completely from the exchange-correlation part.

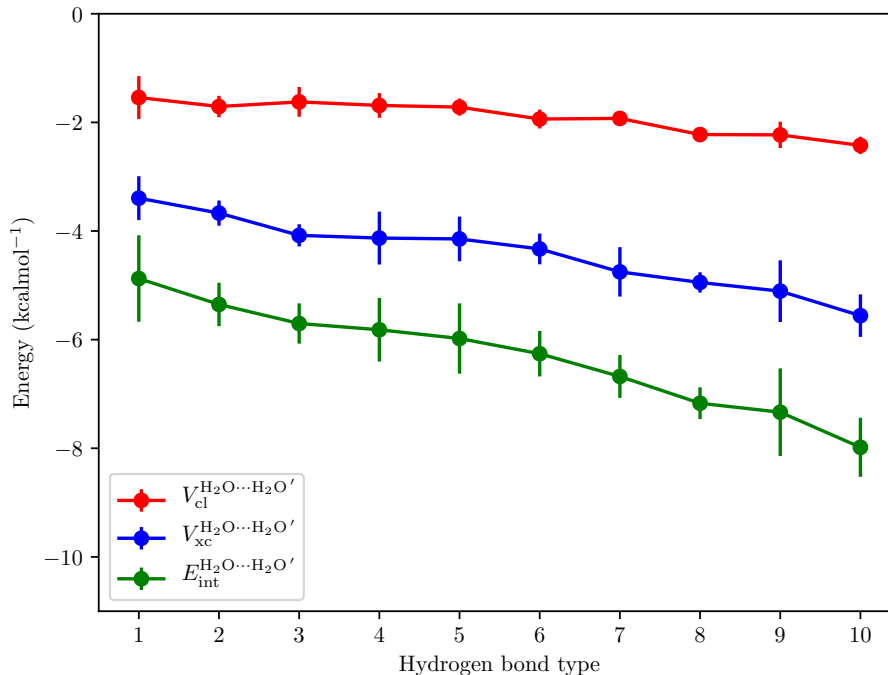


Figure 9: Average values for the classical (blue) and exchange-correlation (red) contributions to the interaction energy (green) for the different types of hydrogen bond put forward in Table 1.

Figure 10 shows the average values of for the DIs between water molecules for the different types of HBs addressed in this paper. Similar to the exchange-correlation term, the DI is a measure of the number of electrons shared between water molecules. The hydrogen bonds with

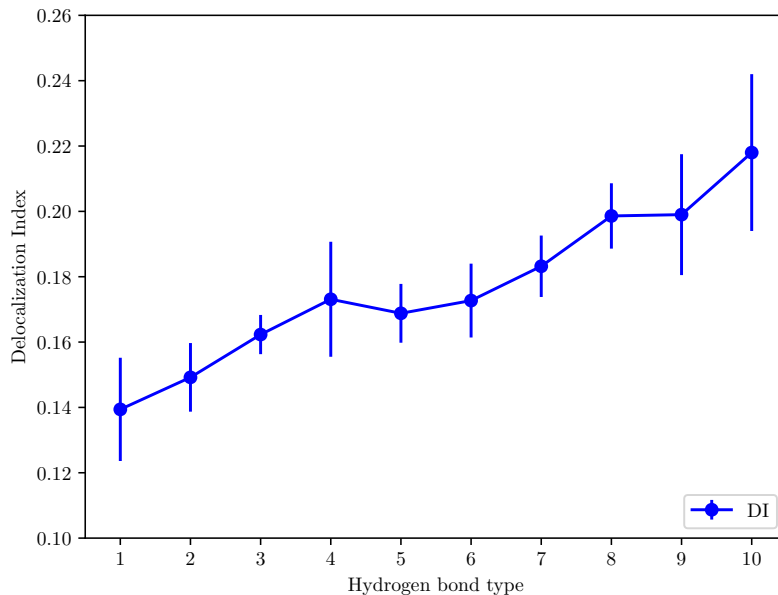


Figure 10: Delocalisation indices between hydrogen-bonded water molecules for different HBs show in Table 1. The values are displayed in atomic units

the largest formation energies have the most sizable number of shared pairs of electrons and therefore of covalency as reflected in the compared value of  $DI^{\text{H}_2\text{O}\cdots\text{H}_2\text{O}}$  and  $E_{\text{xc}}^{\text{H}_2\text{O}\cdots\text{H}_2\text{O}'}$ . There is indeed a strong correlation between these last two mentioned quantities (Figure 11). Such correlation can be exploited by considering that the computational cost of the computation of DIs represents only a fraction of that corresponding to  $E_{\text{xc}}^{\text{H}_2\text{O}\cdots\text{H}_2\text{O}'}$ .

### Concluding remarks

We have used the IQA energy partition to determine the hydrogen bond formation energies in water clusters which encompass tetracoordinated  $\text{H}_2\text{O}$  monomers. This endeavour allowed us to expand our previously reported classification of hydrogen bonds based on HB connectivity within water hexamers to include tetracoordinated water molecules. Our results show that the strongest and weakest HBs are formed by tricoordinated monomers while contacts between tetracoordinated water molecules are on the middle of this scale. The number of available water

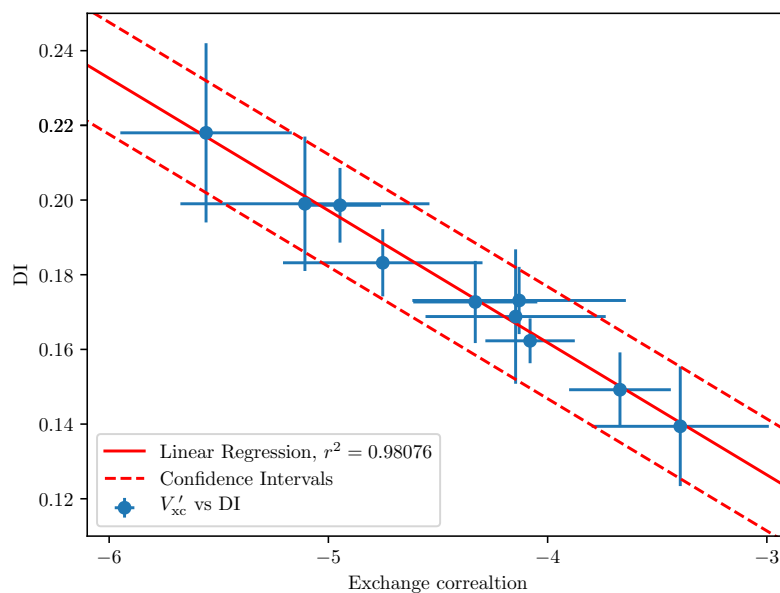


Figure 11: Correlation between exchange-correlation contribution to the hydrogen bond formation energy,  $E_{xc}^{\text{H}_2\text{O}\cdots\text{H}_2\text{O}'}$ , and the delocalisation indices between hydrogen-bonded water molecules for different HBs show in Table 1.

molecules in small water clusters is limited and the system form fewer but stronger HBs. On the other hand, large water clusters contain tetracoordinated water monomers. This possibility (i) reduces HB anticooperative effects which occur due to tricoordinated molecules acting as poor HB donors or acceptors, and (ii) it increases the number of attractive interactions within the system. Altogether, we expect that the analysis presented herein will prove useful to the understanding of the structure and nature of hydrogen-bonded (e.g. water) clusters.

## Acknowledgements

We acknowledge financial support from CONACyT/Mexico (grant 253776) and PAPITT/UNAM (project IN205118). We are also thankful to DGTIC/UNAM for computer time (project LANCAD-UNAM-DGTIC 250). A.M.P. thanks the Spanish MICINN (grant PGC2018-095953-B-I00) the FICYt (grant IDI-2018-000177) and the European Union FEDER funds for financial

support.

## References

- [1] L. Muñoz-Rugeles, A. Galano, J. R. Alvarez-Idaboy, *Phys. Chem. Chem. Phys.* **2017**, *19*, 15296–15309.
- [2] E. Romero-Montalvo, J. M. Guevara-Vela, W. E. Vallejo Narváez, A. Costales, Á. Martín Pendás, M. Hernández-Rodríguez, T. Rocha-Rinza, *Chem. Commun.* **2017**, *53*, 3516–3519.
- [3] J. M. Guevara-Vela, R. Chávez-Calvillo, M. García-Revilla, J. Hernández-Trujillo, O. Christiansen, E. Francisco, Á. Martín Pendás, T. Rocha-Rinza, *Chem. Eur. J.* **2013**, *19*, 14304–14315.
- [4] J. M. Guevara-Vela, E. Romero-Montalvo, V. A. M. Gómez, R. Chávez-Calvillo, M. García-Revilla, E. Francisco, Á. M. Pendás, T. Rocha-Rinza, *Phys. Chem. Chem. Phys.* **2016**, *18*, 19557–19566.
- [5] K. Liu, J. D. Cruzan, R. J. Saykally, *Science* **1996**, *271*, 929–933.
- [6] J. K. Gregory, *Science* **1997**, *275*, 814–817.
- [7] S. S. Xantheas, *Chem. Phys.* **2000**, *258*, 225–231.
- [8] T. Steiner, *Angew. Chem. Int. Ed.* **2002**, *41*, 48–76.
- [9] P. L. A. Popelier in *Intermolecular Forces and Clusters I*, Springer Berlin Heidelberg, **2005**, pp. 1–56.
- [10] P. L. A. Popelier, *Applications of Topological Methods in Molecular Chemistry*, Springer International Publishing, **2016**.
- [11] C. F. Matta, *J. Comput. Chem.* **2010**, *31*, 1297–1311.
- [12] C. Trujillo, G. Sánchez-Sanz, *ChemPhysChem* **2015**, *17*, 395–405.
- [13] M. Alonso, T. Woller, F. J. Martín-Martínez, J. Contreras-García, P. Geerlings, F. De Proft, *Chem. Eur. J.* **2014**, *20*, 4931–4941.
- [14] G. Sánchez-Sanz, C. Trujillo, I. Alkorta, J. Elguero, *ChemPhysChem* **2012**, *13*, 496–503.
- [15] G. Sánchez-Sanz, C. Trujillo, M. Solimannejad, I. Alkorta, J. Elguero, *Phys. Chem. Chem. Phys.* **2013**, *15*, 14310–14318.
- [16] G. Sánchez-Sanz, C. Trujillo, I. Alkorta, J. Elguero, *Phys. Chem. Chem. Phys.* **2014**, *16*, 15900–15909.

- [17] G. Sánchez-Sanz, C. Trujillo, *J. Phys. Chem. A* **2018**, *122*, 1369–1377.
- [18] M. A. Blanco, A. Martín Pendás, E. Francisco, *J. Chem. Theory Comput.* **2005**, *1*, 1096–1109.
- [19] O. A. Syzgantseva, V. Tognetti, L. Joubert, *J. Phys. Chem. A* **2013**, *117*, 8969–8980.
- [20] K. Eskandari, M. Lesani, *Chem. Eur. J.* **2015**, *21*, 4739–4746.
- [21] J. M. Guevara-Vela, D. Ochoa-Resendiz, A. Costales, R. Hernández-Lamoneda, Á. Martín Pendás, *ChemPhysChem* **2018**, *19*, 2512–2517.
- [22] N. Orangi, K. Eskandari, J. C. R. Thacker, P. L. A. Popelier, *ChemPhysChem* **2019**, *20*, 1922–1930.
- [23] K. Eskandari, *Comput. Theor. Chem.* **2016**, *1090*, 74–79.
- [24] J. L. Casals-Sainz, F. Jiménez-Grávalos, A. Costales, E. Francisco, Á. M. Pendás, *J. Phys. Chem. A* **2018**, *122*, 849–858.
- [25] J. L. Casals-Sainz, A. Costales, E. Francisco, Á. Martín Pendás, *Molecules* **2019**, *24*, 2204.
- [26] J. M. Guevara-Vela, E. Romero-Montalvo, A. Costales, Á. Martín Pendás, T. Rocha-Rinza, *Phys. Chem. Chem. Phys.* **2016**, *18*, 26383–26390.
- [27] I. Alkorta, I. Mata, E. Molins, E. Espinosa, *Chem. Eur. J.* **2016**, *22*, 9226–9234.
- [28] O. J. Backhouse, J. C. R. Thacker, P. L. A. Popelier, *ChemPhysChem* **2019**, *20*, 555–564.
- [29] R. F. W. Bader, *Atoms in molecules: A Quantum Theory*, Oxford University Press, **1990**.
- [30] R. F. W. Bader, *Chem. Rev.* **1991**, *91*, 893–928.
- [31] X. Fradera, M. A. Austen, R. F. W. Bader, *J. Phys. Chem. A* **1999**, *103*, 304–314.
- [32] E. Francisco, Á. Martín Pendás, M. A. Blanco, *J. Chem. Theory Comput.* **2005**, *2*, 90–102.
- [33] P. Maxwell, Á. M. Pendás, P. L. A. Popelier, *Phys. Chem. Chem. Phys.* **2016**, *18*, 20986–21000.
- [34] E. Francisco, J. L. Casals-Sainz, T. Rocha-Rinza, A. M. Pendás, *Theor. Chem. Acc.* **2016**, *135*.
- [35] S. Yoo, E. Aprà, X. C. Zeng, S. S. Xantheas, *J. Phys. Chem. Lett.* **2010**, *1*, 3122–3127.
- [36] J. Segarra-Martí, M. Merchán, D. Roca-Sanjuán, *J. Chem. Phys.* **2012**, *136*, 244306.

- [37] A. Rakshit, P. Bandyopadhyay, J. P. Heindel, S. S. Xantheas, *J. Chem. Phys.* **2019**, *151*, 214307.
- [38] Y. Zhao, D. G. Truhlar, *J. Phys. Chem. A* **2006**, *110*, 13126–13130.
- [39] A. D. McLean, G. S. Chandler, *J. Phys. Chem. A* **1980**, *72*, 5639–5648.
- [40] T. H. Dunning, *J. Chem. Phys.* **1989**, *90*, 1007–1023.
- [41] R. A. Kendall, T. H. Dunning, R. J. Harrison, *J. Chem. Phys.* **1992**, *96*, 6796–6806.
- [42] M. J. Frisch, G. W. Trucks, H. B. Schlegel, G. E. Scuseria, M. A. Robb, J. R. Cheeseman, G. Scalmani, V. Barone, B. Mennucci, G. A. Petersson, H. Nakatsuji, M. Caricato, X. Li, H. P. Hratchian, A. F. Izmaylov, J. Bloino, G. Zheng, J. L. Sonnenberg, M. Hada, M. Ehara, K. Toyota, R. Fukuda, J. Hasegawa, M. Ishida, T. Nakajima, Y. Honda, O. Kitao, H. Nakai, T. Vreven, J. A. Montgomery, Jr., J. E. Peralta, F. Ogliaro, M. Bearpark, J. J. Heyd, E. Brothers, K. N. Kudin, V. N. Staroverov, R. Kobayashi, J. Normand, K. Raghavachari, A. Rendell, J. C. Burant, S. S. Iyengar, J. Tomasi, M. Cossi, N. Rega, J. M. Millam, M. Klene, J. E. Knox, J. B. Cross, V. Bakken, C. Adamo, J. Jaramillo, R. Gomperts, R. E. Stratmann, O. Yazyev, A. J. Austin, R. Cammi, C. Pomelli, J. W. Ochterski, R. L. Martin, K. Morokuma, V. G. Zakrzewski, G. A. Voth, P. Salvador, J. J. Dannenberg, S. Dapprich, A. D. Daniels, . Farkas, J. B. Foresman, J. V. Ortiz, J. Cioslowski, D. J. Fox, *Gaussian09 Revision D.01*, Gaussian Inc. Wallingford CT 2009.
- [43] F. Jiménez-Grávalos, J. L. Casals-Sainz, E. Francisco, T. Rocha-Rinza, Á. M. Pendás, J. M. Guevara-Vela, *Theor. Chem. Acc.* **2019**, *139*.
- [44] T. A. Keith, *AIMAll (Version 19.02.13)*, TK Gristmill Software, Overland Park KS, USA, 2019 (aim.tkgristmill.com).
- [45] J. D. Hunter, *Computing In Science & Engineering* **2007**, *9*, 90–95.
- [46] E. Espinosa, E. Molins, C. Lecomte, *Chem. Phys. Lett.* **1998**, *285*, 170–173.
- [47] E. M. Schulson, P. Duval in *Creep and Fracture of Ice*, Cambridge University Press, **2009**, pp. 5–29.
- [48] R. Feistel, W. Wagner, *Geochimica et Cosmochimica Acta* **2007**, *71*, 36–45.